Protoplasma (2020) 257:1667–1683
https://doi.org/10.1007/s00709-020-01535-8

ORIGINAL ARTICLE

Differential impact of some metal(loid)s on oxidative stress, antioxidant system, sulfur compounds, and protein profile of Indian mustard (*Brassica juncea* L.)

Javed Ahmad[1] · Sadia Qamar[1] · Nida[1] · Faheema Khan[2] · Inamul Haq[1] · Asma Al-Huqail[2] · Mohammad Irfan Qureshi[1]

Received: 2 March 2020 / Accepted: 8 July 2020 / Published online: 1 August 2020

Abstract

Levels of arsenic (As), chromium (Cr), and copper (Cu) are increasing in the soils worldwide. Such contaminants cause toxicity in the plant systems which adversely affects growth and productivity. The objective of the present investigation was to elucidate individual and combined effects of As, Cr, and Cu (100 μM each) stress in metal hyper-accumulator plant Indian mustard (*Brassica juncea* L.), exposed for a week. The highest accumulation was in the roots and in decreasing order viz. Cu > As > Cr. The magnitude of oxidative stress was maximal in combined stress, followed by As, Cr, and then Cu stress. Glutathione in conjunction with glutathione reductase, glutathione peroxidase, and glutathione S-transferase increased in all set of stress treatments, notably when exposed to Cr alone. In addition, the level of sulfur-rich compounds like cysteine, phytochelatins, and non-protein thiols increased under each stress indicating efficient coupling of the enzyme system and sulfur-containing compounds during stress conditions. The highest tolerance or growth index of plants was recorded for Cu. Protein profiling of leaf tissues showed modulation of protein patterns in each stress. Mediator of RNA polymerase II transcription subunit 1 isoform X1, RuBisCO (large subunit), and ribosomal protein S3 proteins were more abundant under Cr and Cu stress. Zinc finger A20/AN1 domain-containing stress-associated protein 5–like protein was more abundant under Cu stress. HSP (15.7 kDa) and autophagy protein 5–like were in higher abundance under As and combined stress. Our results suggest that Indian mustard has a differential mode of defense against a particular stressor at the level of protein expression profile.

Keywords Indian mustard · Mass spectrometry · Metal(loid)s · Protein profiling · Sulfur-containing compounds

Asma Al-Huqail and Mohammad Irfan Qureshi contributed equally as corresponding author to this work.

Handling Editor: Néstor Carrillo

Electronic supplementary material The online version of this article (https://doi.org/10.1007/s00709-020-01535-8) contains supplementary material, which is available to authorized users.

✉ Mohammad Irfan Qureshi
mirfanq@gmail.com

Javed Ahmad
javedahmad12@gmail.com

Sadia Qamar
zadiaqamar11@gmail.com

Nida
kausarnida4@gmail.com

Faheema Khan
kfaheema@ksu.edu.sa

Inamul Haq
drihaq@yahoo.com

Asma Al-Huqail
aalhuqail@ksu.edu.sa

[1] Department of Biotechnology, Jamia Millia Islamia, New Delhi 110 025, India

[2] Botany and Microbiology Department, College of Science, King Saud University, Riyadh 11451, Saudi Arabia

Introduction

One of the most critical environmental and health problems arising worldwide is associated with increasing levels of toxic metal and metalloid pollution. Such toxic elements intrude into food chains easily as they have the property of ionization, persistence, and bioaccumulation, for instance, arsenic (As), chromium (Cr), and copper (Cu) (Ali et al. 2019). However, the availability and movement in the plant of any particular metal depend largely on its solubility, type, and pH of soil and the presence of transporters in the roots. Furthermore, it might become more devastating for plants if toxicants are present in a variety. Usually, many toxic elements occur in the soil at a single time and could be attributed to synergistic toxicity on the plants. The availability of multiple types of toxic elements might have different dynamics compared with a single one. Metal interactions at soil cation exchange sites as well as competition at root absorption sites will affect the metal absorption by plant (Muszyńska and Labudda 2019) and plant health as a whole.

Though the coexistence of various metals in the soil is a mainstream event, still less data is available related to plant growth and uptake during combination stress caused by exposure of multiple metals. As a mere fact, industries and urban technologies are leading to a rise in levels of As, Cr, and Cu (Šiukšta et al. 2019). In addition, many pollutants are in high used these days such as chromated copper arsenate (CCA) in wood-preserving industries. These industrial units discharge their effluents into the environment directly and cause the contamination of such resources and ecosystems by metal(-loid)s concomitantly (Safa et al. 2020). Cu being one of the essential micro-nutrients is responsible for plant growth even in low concentration. More increase in the concentration of Cu leads to phytotoxicity resulting into reduced plant growth, misbalancing of nutrient metabolism, enzyme inhibition, decreased rate of photosynthetic, cellular damages, etc. (Gonzaga et al. 2019), whereas As and Cr are non-essential and highly phytotoxic which causes critical biochemical, physiological, and morphological impact impairments (Rahman and Singh 2019).

Therefore, it is interesting to know if the presence of single metal and mixture of metals would cause similar or different levels of reactive oxygen species (ROS) production in cellular compartments and that what sort of differences would be there in damages caused to the plant metabolic and molecular processes. Furthermore, the response of the plant defense system to multiple elemental stress would impart a realistic scenario that usually occurs in the natural soils.

This is well documented that a group of enzymes called lipoxygenases (LOX) catalyzes, more active under stress, addition of oxygen to polyunsaturated fatty acids (PUFA) including linoleic acid and linolenic acid. LOX initiates the synthesis of traumatin, jasmonic acid (JA), and methyl jasmonate (MeJA), collectively known as oxylipins which are acyclic or cyclic compounds. The phyto-oxylipins activate the gene expression that improves the plant defense against stress (Thakur and Udayashankar 2019).

However, as a key constituent of the antioxidant defense system, the glutathione (GSH) and their associated enzymes such as glutathione reductase (GR), glutathione peroxidase (GPX), and glutathione S-transferase (GST) collectively defend plant against reactive oxygen species (ROS) generated through oxidative stress via metal toxicity (Paul et al. 2019). Moreover, a network of other sulfur-containing compounds like cysteine (Cys), phytochelatins (PCs), and non-protein thiols (NPTs) contribute significantly to the detoxification process (Lu et al. 2019). In addition, total proteins are important functional components in stress resilience of plants though such are the preferred site attacked by ROS. Therefore, the modulation of protein pattern is also crucial under metal stress (Baig et al. 2018).

Indian mustard (*Brassica juncea* L.) is widely used as oilseed and vegetable in the Indian northern region (Ahmad et al. 2009, 2012). Besides this, *B. juncea* has special consideration due to its significance in studying the heavy metal tolerance mechanisms (Qureshi et al. 2010; Niazi et al. 2017; Rizwan et al. 2018). *Brassica juncea* is considered a good candidate for tolerating high concentrations of toxic elements. Many studies have shown that this plant has efficient mechanisms to counter metal stress, oxidative stress, and compartmentalization of the metals (Qadir et al. 2004). In addition, it is a fast-growing, high biomass-producing, and less water-requiring plant with high metal removal efficiency from the soil (Su et al. 2018). Furthermore, *B. juncea* is appropriate for the assessment of individual and combined toxicity as it encounters the real environment pollution in the field; therefore, it is used as plant material in this case. Hence, the purpose of the present investigation was to study the impact of individual stressors As, Cr, and Cu and their combined stress on the growth, level of oxidative stress, metal(loid) accumulation, protein profile, content of sulfur-containing compounds, and activity of glutathione-associated enzymes in *B. juncea*.

Materials and methods

Plant material and stress conditions

Brassica juncea L. cultivar Pusa Jai Kisan was used in the present study. Seeds were procured from the Indian Agriculture Research Institute (IARI), New Delhi, India. A total of 100 g of seeds was surface-sterilized by 0.1% $HgCl_2$ for 60 s then washed ten times with deionized water, followed by germination on a wet paper towel at 25 °C under dark conditions. Five-day-old seedlings were transferred to the beakers (5 seedlings/250 mL, supported by aluminum foil net)

having a Hoagland nutrient solution of half-strength, pH 5.6 (Hoagland and Arnon 1950) and kept further in a plant culture chamber with a light intensity of about 200 μmol m^{-1} s^{-1} of 16 h a day and night temperature of 28/25 °C and relative humidity of 55 to 75%, respectively. Thirty-day-old plants were exposed to As (Na_3AsO_4), Cr ($K_2Cr_2O_7$), and Cu ($CuNO_3$), 100 μM of each separately as well as combined (100 μM As + 100 μM Cr + 100 μM Cu). Treatment was given once through the Hoagland nutrient solution for the duration of 7 days. One set of plants was fed with stressor-free nutrients, served as control. At 7 days after the treatment (DAT), samples were collected, rinsed with deionized distilled water, and utilized for numerous physiological and biochemical studies immediately. Representative plants from treated sets of *B. juncea* are presented in the Supplementary Information (Fig. S1). The study was carried out in a completely randomized plan with three replicates. All data are mean of triplicates (± S.E).

Growth and tolerance index

Fresh weights (g) of shoots and roots were recorded separately. To determine the accumulation of dry matter of plant material, shoots and roots were desiccated at 62 °C in a hot air oven for 2 days. Plant dry was recorded to calculate the dry matter and presented in grams per plant. The tolerance index (TI) was estimated through the division of the root length of the plant exposed to individual As, Cr, and Cu and their combined stress to the root length measured under control condition. The following equation was used for the calculation of the tolerance index.

$$\text{Tolerance index}(\%) = \frac{\text{Root length in metal treatment}}{\text{Root length under control condition}} \times 100$$

Investigation of metal accumulation, translocation factor, and bioconcentration factor

Every plant was cleaned with the help of distilled water to eliminate the dust particles and residual part of the Hoagland solution. Fresh plant parts (shoots and roots) were kept in an oven at 70 °C/48 h for complete desiccation. In the Kjeldahl assembly, 0.5 g of plant material was digested in 100 mL of a mixture (5:2) containing concentrated HNO_3 and $HClO_4$. Resultant was boiled in a hood and bleached with drops of hydrogen peroxide occasionally till it got clear. The digest was cooled and then filtered using Whatman no. 1 filter paper. The volume of the filtrates was made to 50 mL and used for the estimation of toxic metals (As, Cr, and Cu) through ICP-OES (inductively coupled plasma - optical emission spectrometry). The translocation factor (TF) was calculated with shoot and root metal concentrations to determine the relative mobilization of metal from root to shoot as the method given by Marchiol et al. 2004.

$$\text{Translocation factor} = \frac{\text{Metal content in shoots}}{\text{Metal content in roots}}$$

The bioconcentration factor (BCF) of As, Cr, and Cu from the Hoagland solution or culture media to plants was calculated by using the formula as below.

$$\text{BCF}_{\text{Roots}} = \frac{\text{Metal concentration in roots}}{\text{Metal concentration in culture media}}$$

$$\text{BCF}_{\text{Shoots}} = \frac{\text{Metal concentration in shoots}}{\text{Metal concentration in culture media}}$$

Estimation of oxidative stress

Histochemical localization of free radicals

Accumulation of hydrogen peroxide (H_2O_2) and superoxide ($O_2^{\bullet-}$) was assessed chemically by DAB (3, 3′-diaminobenzidine) and NBT (nitro blue tetrazolium) staining of *B. juncea* leaves as per the procedure illustrated by Scarpeci et al. (2008).

Hydrogen peroxide visualization

Leaves were placed overnight in a DAB solution (1 mg mL^{-1}) at pH 3.8. Later, the green pigment was removed from the leaves by boiling them in the ethanol solution for about 10 min. Reddish-brown pigmentation got visible denoting the presence of the H_2O_2 which was further visualized and then digitized.

Superoxide visualization For $O_2^{\bullet-}$ detection, the leaves were floated in 50 mM solution of Na_3PO_4 at pH 7.4 having NBT 0.2% for 2 h. The interaction of NBT with $O_2^{\bullet-}$ resulted in insoluble formazan which was then visualized in leaf as dark blue–colored spots after removal of chlorophyll by boiling in ethanol solution for 10 min followed by digitization of blue spots.

TBARS content

The intensity of oxidative stress was estimated using the method of Heath and Packer (1968) in the leaf by quantification of thiobarbituric acid reactive substances (TBARS) which are the by-products of oxidative stress degradation of biomolecules. One gram of leaf sample was weighed and crushed in liquid nitrogen followed by the addition of 10 mL 1% (w/v) trichloroacetic acid (TCA). The mixture was vigorously shacked and spun at 10,000 rpm/5 min/4 °C. About 1 mL

supernatant was transferred to fresh tubes and added with 4 mL of 0.5% (w/v) TBA which was boiled at 99 °C for 30 min. This mixture was ice-cooled and centrifuged again at 5500 rpm/5 min. At 532 nm, the supernatant optical density was noted and then modified for non-specific turbidity through deducting the value from the 600-nm absorbance. The units were kept in nmol g^{-1} FW.

Activity of lipoxygenase

The activity level of lipoxygenase (LOX) was evaluated using the procedure of Doderer et al. (1992). The reaction mixture (linoleic acid plus 50 μL Tween 20 in 0.1 M phosphate buffer, pH 6.5) was mixed with 20 μL of enzyme extract and enzyme kinetics was performed. The reaction mixture without a substrate solution was used as the control. LOX activity was calculated observing the rise of absorbance at the 234 nm by substrate linoleic acid. With the help of an extinction coefficient of 25 mM^{-1} cm^{-1}, the activity was calculated and enzyme unit was represented as 1 nmol of oxidized substrate min^{-1} mg^{-1} protein.

Estimation of cysteine content

The cysteine concentration was evaluated as the protocol given by Gaitonde (1967). In this method, 1 mL of the sample was made by the blending of leaf tissue with 5% perchloric acid, acetic acid, and ninhydrin acid then mixed well. After that, the sample mixture was heated for 10 min then quickly chilled under cold water. The sample was diluted to make 5 mL of final volume with 90% C_2H_5OH and optical density was recorded at 560 nm. The standard curve of L-cysteine (Himedia Laboratories, India) was prepared to calculate the actual value of cysteine in samples.

Glutathione estimation

The content of different forms of glutathione (GSSG, GSH, and GSH + GSSG) was assessed by the protocol of Anderson et al. (1985) through a GR-catalyzed reaction. Leaf material (0.5 g) was homogenized using 2 mL of 5% 5-sulphosalcylic acid to run the GSH oxidation. Then, the test mixture (without leaf extract and GR) was calibrated for about 5 min at 30 °C. The absorbance was recorded at 412 nm after the addition of leaf extract. The blank was made by substituting the leaf extract with 5% 5-sulphosalcylic acid. Now in a similar vial, 50 μL of 0.4% (w/v) NADPH and 0.2 units per assay GR were supplemented. Next, the reaction was performed at 412 nm/30 min/25 °C and the absorbance was recorded for total glutathione content. The substantial value of glutathione content was calculated against the standard curve of GSH (10–100 nmol) and mentioned as nmol g^{-1} FW.

Extraction and assays of glutathione-associated enzymes

Leaf material (0.5 g) was homogenized in 5 mL of chilled phosphate buffer (100 mM, pH 7.4, 2.5 mM D_L-dithiothreitol, 1 mM EDTA, 4% w/v insoluble polyvinyl polypyrolidone, and 0.5% Triton X-100). Next, the homogenate was centrifuged at 10,000 rpm/30 min. In total, 100 μL/mL aliquot was used assay enzyme activities. Extraction of enzymes was performed at 4 °C and all enzymatic evaluations were done at a temperature of 25 °C for 5 min.

Glutathione reductase assay

Glutathione reductase (GR) assay was carried out as described by Foyer and Halliwell (1976). The assay was started by mixing of 100-μL enzyme extract to 0.9 mL of the assay mixture containing K-phosphate buffer (100 mM, pH 7.2, 0.2 mM NADPH, and 0.02 mM GSSG). The intensity of the reaction was evaluated via glutathione-mediated NADPH oxidation marked by a decrease in absorbance at 340 nm. Corrections were made for any GSSG oxidation in the absence of NADPH. The glutathione reductase activity was estimated using an extinction coefficient of 6.2 mM^{-1} cm^{-1}.

Glutathione S-transferase assay

The activity of glutathione S-transferase (GST) was evaluated as the protocol used by Habig et al. (1974) using substrate CDNB (1-choloro-2,4-dinitrobenzene). The glutathione S-transferase (GST) activity was examined in an assay mixture having 1.65 mL of 0.1 M phosphate buffer at pH 6.5, 100 μL of CFE (cell-free extract), 50 μL of 1 mM fresh CDNB (2.025 mg in 5 mL of absolute alcohol), and 0.2 mL of 1 mM GSH (freshly prepared by mixing 3.07 mg in 0.1 M phosphate buffer/10 mL, pH 6.4). The assay mixture was vortex-mixed and the volume was adjusted 20 mL using ultrapure water. Optical density following CDNB was read at 340 nm at an interval of 30 s for about 5 min. The activity of enzyme was presented in nmol of conjugated CDNB produced min^{-1} mg^{-1} of protein using a 9.6×10^3 M^{-1} cm^{-1} M extinction coefficient.

Glutathione peroxidase activity

The activity of glutathione peroxidase (GPX) was measured using H_2O_2 as a substrate in the reaction buffer (100 mM K-phosphate buffer, pH 7.0, 1 mM EDTA, 1 mM NaN_3, 0.12 mM NADPH, 2 mM GSH, 1 unit GR, 0.6 mM H_2O_2, and 50 μl enzyme extract); blank values, without enzyme extract, were deducted from the samples optical density. The shift in optical density at 340 nm for NADPH oxidation was read and used as illustrated by Elia et al. (2003).

Non-protein thiols

The non-protein thiol (NPT) concentration in leaf samples was estimated by the protocol of Howe and Merchant (1992) using Ellman's reagent and a standard curve was prepared by GSH (Sigma-Aldrich, USA) to determine NPTs in leaf tissues. The concentration of NPTs was represented as nmol g^{-1} FW.

Phytochelatins

Phytochelatin (PC) concentration in the leaf sample was estimated by deducting the quantity of GSH from the quantity of total NPTs and presented as nmol g^{-1} FW.

$$\text{Phytochelatin}\left(\text{nmol g}^{-1}\text{FW}\right) = \text{Non protein thiol} - \text{total glutathione}$$

Protein extraction from leaf

The total protein of leaf was isolated and processed as stated by Watson et al. (2003). Leaf tissues were harvested, immediately washed, blot-dried, weighed, and frozen in liquid nitrogen. Frozen leaf samples were powdered in liquid nitrogen and homogenized in Tris-HCl buffer (40 mM, pH 7.4) consisting of EDTA (2 mM), β-mercaptoethanol (0.07%), PVP (2%), PMSF (1%), and Triton X 100 (1%). The homogeneous mixture was centrifuged at 20,000 rpm at 4 °C/1 h. The liquid supernatant was transferred to a new tube then blended with TCA (10%, prepared in acetone) and β-mercaptoethanol (0.07%), and kept at − 20 °C/overnight. Subsequently, chilled mixture of the sample was then centrifuged at 15,000 rpm at 4 °C/15 min. A pellet was collected and washed chilled acetone containing β-mercaptoethanol (0.07%) and EDTA (2 mM). Pellet was further kept in chilled acetone for 5 h and then dried by vacuum. The pellet was processed using 2D cleanup kit (ReadyPrep™, Bio-Rad, USA). This was performed to remove and high-abundance proteins and enrich low-abundance proteins. Finally, recovered protein was used for SDS-PAGE protein profile experiment. The bands with identification of a single protein have been presented and discussed.

SDS-PAGE protein profile

Protein profile pattern was studied using SDS-PAGE by the method of Laemmli (1970). The solubilization buffer consisting of 1.0 mM Tris HCl (pH 6.8), 1.5% SDS, and 2.5 mL β-ME was used to dissolve the pellet. Then, solubilized proteins were estimated by the Bradford reagent using bovine serum albumin (BSA) standard curve. In total, 40 μg of protein was loaded on each well of 12% (w/v) arylamide in a vertical electrophoretic cell (Bio-Rad, USA) at 100 V. After completion of electrophoresis, the acrylamide gels were separated from the unit and rinsed 3 times with autoclaved DW. After that gels were kept overnight in Blue Silver or colloidal CBB (Candiano et al. 2004) stain that contains 10% (v/v) O-phosphoric acid, 10% (w/v) ammonium sulfate, and 0.12% (w/v) CBB-G250 in methanol for proteins staining. After the staining procedure, the gels were kept in autoclaved DW for de-staining until the gels' background turns into stainless and protein bands were apparently visible. Gel images were digitized through the Gel Documentation System (Bio-Rad, USA) for additional study. The image analysis was carried out with image Lab™ software (Bio-Rad, USA) to study the relative shift in the protein profile of different samples. For molecular weight reference, a broad range protein marker (Bangalore Genei, India) was used falling in the range between 14.0 and 97.0 kDa.

In-gel digestion and protein identification

For trypsin digestion of proteins, the protein bands of concern were cut from the gel as a small gel slice using a sterile blade and transferred to a PCR tube. In total, 200 μl of ultrapure water was added to the gel pieces for the purpose of washing. The step was completed by centrifugation at 1100 rpm for 20 min. The washing step was repeated once. A total of 200 μL of 50% (v/v) acetonitrile (ACN) was transferred to the tubes followed by centrifugation at 1100 rpm at 22 °C for 20 min. The ACN treatment step was repeated once. The next step involved mixing 5 μL DTT (1 M) and 49.5 μL NH_4HCO_3 (20 mM) and incubation at 56 °C in ACN. ACN was discarded followed by the addition of approximately 40 μL iodoacetamide (IAA) (55 mM). Centrifugation was done at 1100 rpm at 22 °C and IAA was discarded. Fifty percent (v/v) ACN was again added and centrifuged at 1100 rpm at 24 °C. ACN was removed, and tubes were added with 100% (v/v) ACN followed by centrifugation at 1100 rpm for 20 min. The contents of the tube obtained in the form of a pellet were vacuum-dried. The samples were digested by incubation of the same at 37 °C overnight with 20 μL of 1% (w/v) trypsin made in 20 mM NH_4CO_3. After the digestion of proteins was done, the samples were centrifuged at 1100 rpm for 20 min and the supernatant was carefully transferred to a fresh tube. The supernatant was added with 1% TFA prepared in 50% (v/v) ACN thereby usable for mass spectrometry study. Small peptides obtained by tryptic digestion or the peptide mass fingerprints of the proteins that are differentially expressed were investigated on an ABI 4800 MALDI-TOF/TOF MS Analyzer (Applied Biosystems, USA). Protein identification was done by the ABI GPS Explorer software, version 3.5 (Applied Biosystems, USA), the result-dependent study. Some of the

essential parameters set were as follows: A few important parameter settings used are mentioned herein: Digestion enzyme-trypsin with one missed cleavage; MS (precursor-ion) peak filtering: 800 ± 4000 m/z interval; monoisotopic; minimum (S/N) signal-to-noise ratio 10; mass tolerance approximately 50 ppm. MS/MS peak filtering (fragmentation): monoisotopic, adduct MH+, S/N - minimum, MS/MS fragmentation tolerance approximately 0.2 Da; database used: Viridiplantae, green plants from NCBI database. Contaminants database was also selected. The initial MS scan data was analyzed as peptide mass fingerprinting (PMF) and the proteins were identified by searching against the database using the MASCOT (Matrix Science, (http://www.matrixscience.com) software. For correct protein identification and result elucidation, proteins with high scores were considered keeping in view their theoretical molecular weights.

Statistical analysis

All data were given as the mean ± standard error (SE). The analyses were made by 3 replicates for each parameter studied. The statistical studies were done by using ANOVA (two-way ANOVA) in Instat 3 (GraphPad Instat, San Diego, CA) to assess significant changes at $P \leq 0.05$ and $P \leq 0.01$ (Tukey's post hoc test applied for multiple comparisons). For partial least squares discriminant analysis (PLS-DA) and to calculate the principal component analysis (PCA), the MetaboAnalyst 3.0 software (Xia et al. 2015) was used in the present study. Percent (%) change in comparison with control has been presented in the parentheses.

Results

Effect of metal(loid)s on *B. juncea* growth and tolerance index

A decrease in fresh weight was recorded in shoots of *B. juncea* from 3.76 (control) to 3.08 (− 18%), 3.31 (− 12%), 3.39 (− 10%), and 2.86 (− 24%) grams per plant at 7 DAT in As, Cr, and Cu and their combined stress, respectively (Fig. 1a). A drop in fresh weight was detected in the roots of *B. juncea* from 0.39 to 0.31 (− 20%), 0.33 (− 15%), 0.33 (− 15%), and 0.29 (− 26%) grams per plant at 7 DAT in As, Cr, and Cu and their combined stress respectively, compared with the control plants (Fig. 1b).

A decrease in dry weight was recorded in shoots of *B. juncea* from 0.268 (control) to 0.228 (− 15%), 0.238 (− 11%), 0.241 (− 10%), and 0.21 (− 22%) grams per plant at 7 DAT in individual As, Cr, and Cu and their combined stress, respectively (Fig. 1c). A drop in dry weight was detected in

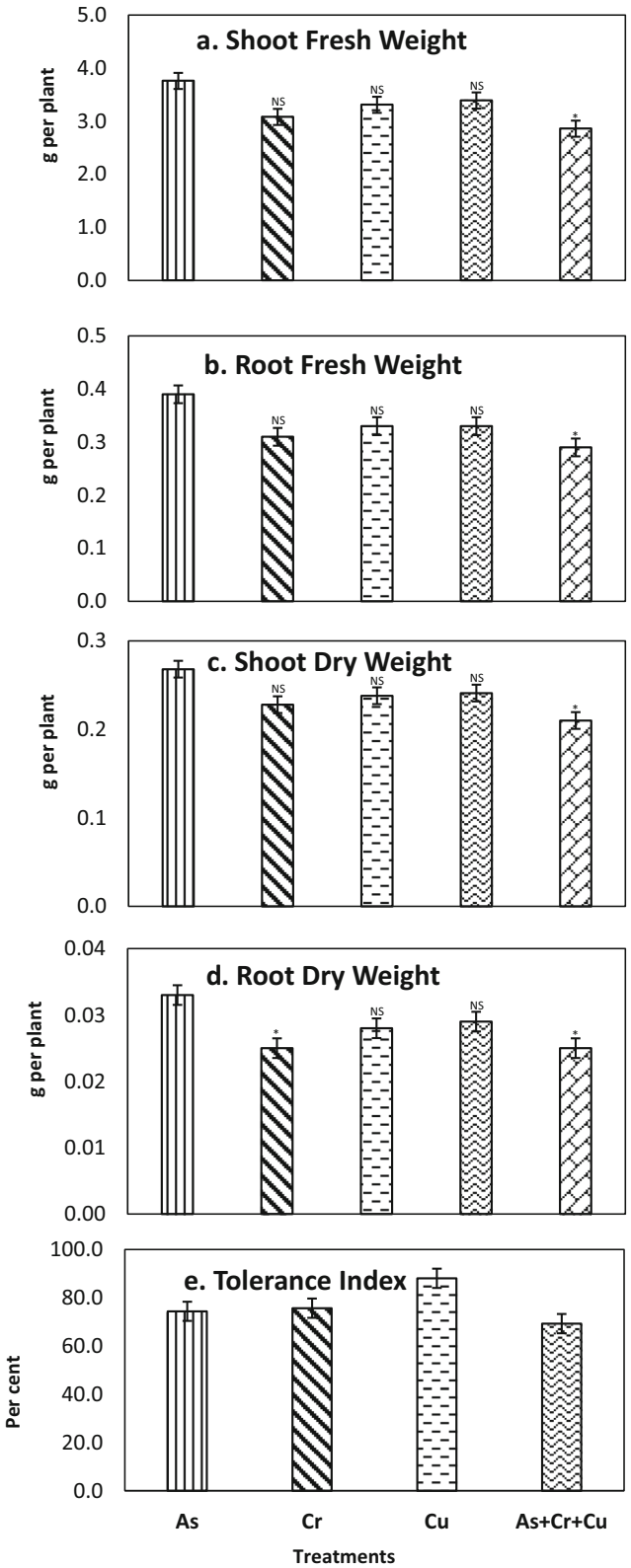

Fig. 1 Changes in the fresh weight of shoots (**a**) and roots (**b**) and dry weight of shoots (**c**) and roots (**d**) and tolerance index (**e**) at 7 days after the treatment (DAT) in *Brassica juncea*. Values are mean of triplicates (± S.E), $^{**}P \leq 0.01$, $^{*}P \leq 0.05$; NS, non-significant

the roots of *B. juncea* from 0.033 (control) to 0.25 (− 24%), 0.28 (− 15%), 0.29 (− 12%), and 0.25 (− 24%) grams per plant at 7 DAT under As, Cr, and Cu and their combined stress, respectively (Fig. 1d).

The tolerance index (TI), based on root elongation in response to the exposure of As, Cr, and Cu and their combined stress, is presented in Fig. 1e. The TI was the highest in the plants grown in Cu-treated Hoagland solution compared with As and Cr and their combined treatments to the Hoagland solution. The lowest tolerance index was reported in combined stresses (As + Cr + Cu) plants at 7 DAT. The trend of tolerance index for As, Cr, and Cu stress in *B. juncea* was TI $(88.1)_{Cu}$ > TI $(75.7)_{Cr}$ > TI $(74.4)_{As}$ > TI $(69.3)_{As+Cr+Cu}$ (Fig. 1e).

Metal(loid) content analyses, translocation factor, and bioconcentration factor

The metal(loid)s' (As, Cr, and Cu) accumulation pattern by *B. juncea* at 7 DAT is given in Table 1. Plant roots showed more accumulation of Cu than of As and Cr at the same concentration and exposure period for individual and their combined stress. A maximum accumulation of 19,140 μg Cu g^{-1} DW was observed for Cu stress while it decreased to 13,020 μg g^{-1} DW for the combination set at 7 DAT in roots. However, an accumulation of 2000 μg g^{-1} DW of As and 1100 μg g^{-1} DW of Cr was recorded for combination set while it was reduced to 1256 μg g^{-1} DW and 896 μg g^{-1} DW in roots respectively for the stress exposure at 7 DAT. The accumulation of As, Cr, and Cu was lower in the shoots compared with that in the roots of *B. juncea*. A maximum accumulation of 636 μg g^{-1} DW of Cr and 572 μg g^{-1} DW of As was observed for combination set while it was 152 μg g^{-1} DW and 38 μg g^{-1} DW, respectively, in the shoots for the stress exposure at 7 DAT. An accumulation of 114 μg g^{-1} DW of Cu was recorded for stress exposure, whereas it was 62 μg g^{-1} DW for combination set in shoots at 7 DAT.

TF > 1 and TF < 1 indicate the high and low ability of plants, respectively, to translocate metals from the roots to shoots. TF values were found to be < 1 in *B. juncea* under all treatment of metal(loid)s (Table 1). For the assessment of *B. juncea*'s potential to remove from the media and accumulate As, Cr, and Cu in the roots and shoots, a bioconcentration factor (BCF) was calculated (Table 1).

BCF values of As were 0.30 and 0.48 in roots and 0.009 and 0.13 in shoots for individual and combination set at 7 DAT, respectively. BCF values of Cr were 0.152, 0.187 in roots and 0.025, 0.108 in shoots for individual and combination set at 7 DAT, respectively. On the other hand, BCF values of Cu were 5.06, 3.47 in roots and 0.030, 0.016 in shoots for individual and combination set at 7 DAT, respectively (Fig. 2).

Oxidative stress–related parameters

Histochemical localization of superoxide ($O_2^{\cdot-}$) anions and hydrogen peroxide (H_2O_2)

The superoxide anions are major oxidant groups accountable to convert NBT to formazan which is insoluble form, which is observable in the leaves as dark blue deposits. Numerous blue deposits were detected in metal-treated plants. The accumulation of $O_2^{\cdot-}$ was the highest in the leaf of combined stress treatment followed by Cr-, As-, and Cu-treated plants. However, certain blue deposits are also shown by control plants, demonstrating the production of superoxide radicals in standard conditions of growth (Fig. 2a–e). Similarly, accumulation of H_2O_2 was visually detected successfully in terms of H_2O_2-catalyzed polymerization of 3, 3-aminobenzidine

Table 1 Impact of As, Cr, and Cu and their combined stress on metal(loid) content, translocation factor values (TF values), and bioconcentration factor values (BCF values) in *B. juncea* at 7 days after treatment (DAT)

Treatment (μM)	Metal Accumulation		TF	BCF	
	Root	Shoot		Root	Shoot
As concentration (μg g^{-1} DW)					
As (100 μM)	1256	152	0.12	0.30	0.009
As (100 μM) + Cr (100 μM) + Cu (100 μM)	2000	572	0.28	0.48	0.13
Cr concentration (μg g^{-1} DW)					
Cr (100 μM)	896	38	0.042	0.152	0.025
As (100 μM) + Cr (100 μM) + Cu (100 μM)	1100	636	0.57	0.187	0.108
Cu concentration (μg g^{-1} DW)					
Cu (100 μM)	19,140	114	0.005	5.06	0.030
As (100 μM) + Cr (100 μM) + Cu (100 μM)	13,020	62	0.003	3.47	0.016

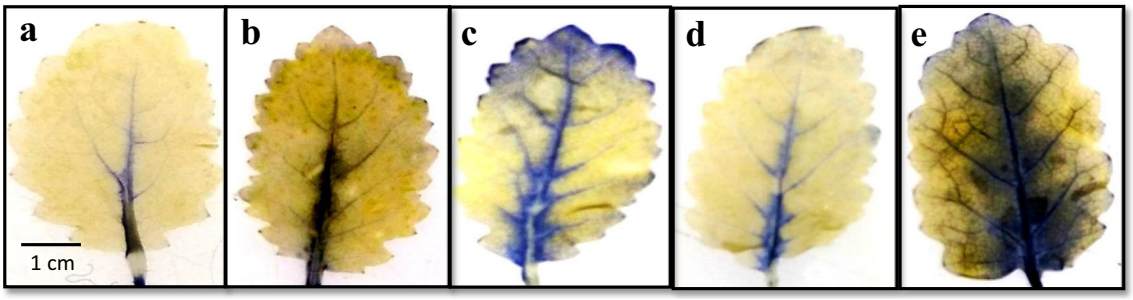

Fig. 2 Dark blue formazan of superoxides produced in NBT-stained leaves of *Brassica juncea* at 7 DAT. **a** Control (0.0 μM metals), **b** arsenic (As, 100 μM), **c** chromium (Cr, 100 μM), **d** copper (Cu, 100 μM), and **e** combined stress (As, 100 μM + Cu, 100 μM + Cr, 100 μM). The experiment was conducted three times

(DAB) characterized by a brown precipitate (Fig. 3a–e). The area and intensity of brown coloration were more in combined and arsenic stressed plants. The occurrence of H_2O_2 was intermediate in Cr- and Cu-treated plants.

TBARS content

The concentration of TBARS indicates the oxidative stress level in *B. juncea* exposed to As, Cr, and Cu and their combined stress. When compared with the control plants, As, Cr, and Cu and their combined (As + Cr + Cu) stress increased the TBARS level from 3.6 nmole g^{-1} FW to 6.1 (+ 69%), 5.3 (+ 44%), 4.8 (+ 33%), and 6.9 (+ 80%) nmole g^{-1} FW in *B. juncea* at 7 DAT respectively (Fig. 4a).

LOX activity

Besides oxylipins, LOX is also involved in the formation of malondialdehyde (MDA). In the treatment of As, Cr, and Cu stress, LOX activity amplified from 5.6 to 8.4 EU min^{-1} mg^{-1} protein (+ 50%), 5.6 to 9.4 EU $min^{-1}mg^{-1}$protein (+ 67%), and 5.6 to 7.8 EU min^{-1} mg^{-1} protein (+ 39%) at 7 DAT, respectively. However, in combined (As + Cr + Cu) stress, LOX showed more activity, increased from 5.6 EU (control) to 11.1 EU min^{-1} mg^{-1} protein (+ 98%) (Fig. 4b).

Cysteine and glutathione content

Under the exposure of As, Cr, and Cu stress, cysteine content increased from 0.16 to 0.20 μmole g^{-1} FW (+ 25%), 0.16 to 0.21 μmole g^{-1} FW (+ 31%), 0.16 to 0.22 μmole g^{-1} FW (+ 38%) at 7 DAT, respectively, compared with the control. However, in combined stress (As + Cr + Cu), cysteine increased from 0.16 to 0.19 μmole g^{-1} FW (+ 19%) (Fig. 5a). The concentration glutathione (reduced, GSH), (oxidized, GSSG), and total glutathione (GSSG+GSH) got increased in all metal-treated samples over control. In As-treated plants, forms of glutathione (reduced, oxidized, and total) content increased from 44.5 to 68.1 nmole g^{-1} FW (+ 53%), 12.5 to 16 nmole g^{-1} FW (+ 28%), and 57.0 to 84.2 nmole g^{-1} FW (+ 47%), respectively, at 7 DAT. This increase was more prominent under Cr stress, which was increased from 44.5 to 71.3 nmole g^{-1} FW (+60%), 12.5 to 18.2 nmole g^{-1} FW (+ 46%), and 57.0 to 89.5 nmole g^{-1} FW (+ 57%), in GSH, GSSH, and total glutathione content, at 7 DAT. Cu stress imparted inflation about 44.5 to 65.1 nmole g^{-1} FW (+ 46%), 12.5 to 18.2 nmole g^{-1} FW (+ 47%), and 57 to 83.4 nmole g^{-1} FW (+ 46%) for the GSH, GSSG, and also for total glutathione content (GSH + GSSG) (Fig. 6a). The rise in these values was less prominent in combined stress and were varied from 44.5 to 50.2 nmole g^{-1} FW (+ 13%), 12.5 to 15.0 nmole g^{-1} FW (+ 16.6%), and 57.0 to 65.9 nmole g^{-1} FW (+ 16%) for GSH reduced form, GSSG, and total glutathione (GSH + GSSG), respectively (Fig. 5b).

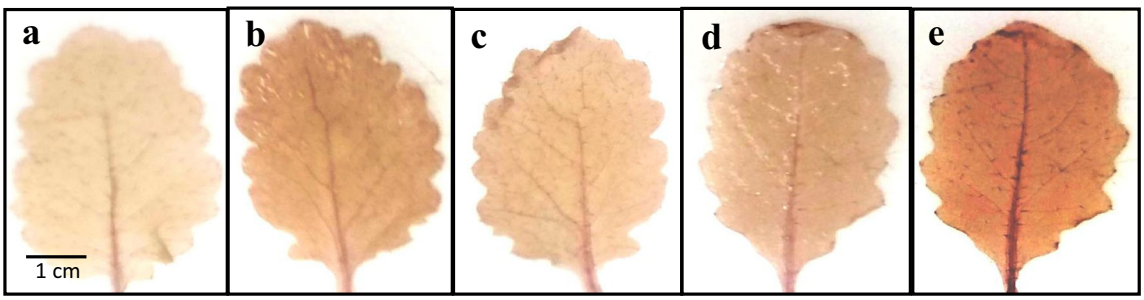

Fig. 3 Brown precipitate formation of hydrogen peroxides in DAB-stained leaves of *Brassica juncea* at 7 DAT. **a** Control (0.0 μM metals), **b** arsenic (As, 100 μM), **c** chromium (Cr, 100 μM), **d** copper (Cu, 100 μM), and **e** combined stress (As, 100 μM + Cu, 100 μM + Cr, 100 μM). The experiment was conducted three times

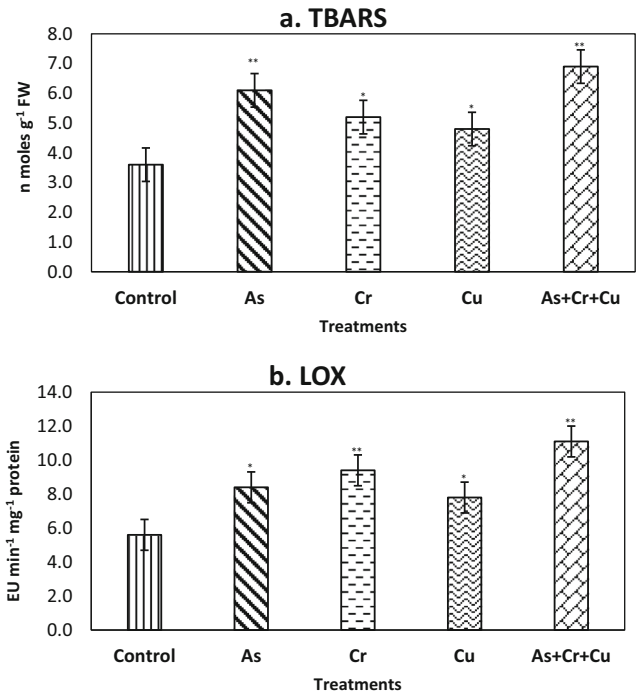

Fig. 4 Changes in the amount of **a** thiobarbituric acid reactive substance (TBARS) and activity of **b** lipoxygenase (LOX) at 7 days after treatment (DAT) in *Brassica juncea*. Values are mean of triplicates (± S.E), $*P \leq 0.05$, $**P \leq 0.01$

Glutathione reductase, glutathione peroxidase, and glutathione S-transferase activities

In the plants treated with As, Cr, and Cu and their combined stress, GR activity increased from 8.8 (control) to 17.0 EU min^{-1} mg^{-1} protein (+ 93%), 8.8 to 19.6 EU min^{-1} mg^{-1} protein (+ 122%), 8.8 to 24.1 EU min^{-1} mg^{-1} protein (+ 173%), and 8.8 to 14.7 EU min^{-1} mg^{-1} protein (+ 67%) at 7 DAT, respectively (Fig. 6a), whereas GPX activity increased from 5.8 (control) to 7.6 EU min^{-1} mg^{-1} protein (+ 31%), 5.8 to 9.5 EU min^{-1} mg^{-1} protein (+ 63%), 5.8 to 8.7 (EU min^{-1} mg^{-1} protein) + 50%, and 5.8 to 7.4 EU min^{-1} mg^{-1} protein (+ 27%) at 7 DAT, respectively (Fig. 6b). The activity of glutathione S-transferase also increased in metal-exposed plants than in control plants. In the case of As, Cr, and Cu and their combined stress, the activity of GST increased from 18.7 (control) to 27.1 EU $min^{-1}mg^{-1}$protein (+ 45%), 18.7 to 35.9 EU min^{-1} mg^{-1} protein (+ 92%), 18.7 to 38.3EU min^{-1} mg^{-1} protein (+ 105%), and 18.7 to 25.5 EU min^{-1} mg^{-1} protein (+ 36%) at 7 DAT, respectively (Fig. 6c).

PC and NPT contents

The PC concentration (phytochelatins = non-protein thiols − total glutathione) increased in each treatment of metals at 7 DAT. The exposure of As, Cr, and Cu and their combined

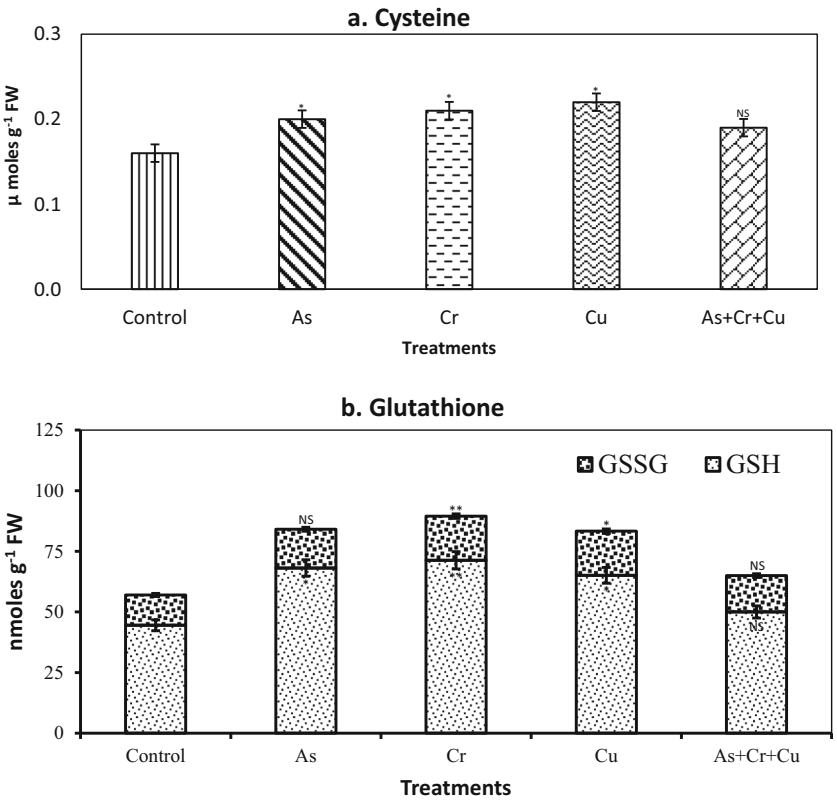

Fig. 5 Changes in the content of **a** cysteine (Cys) and the contents of **b** reduced glutathione (GSH) and oxidized glutathione (GSSH) under different metal stresses. Values are mean of triplicates (± S.E), $*P \leq 0.05$, $**P \leq 0.01$; NS, non-significant

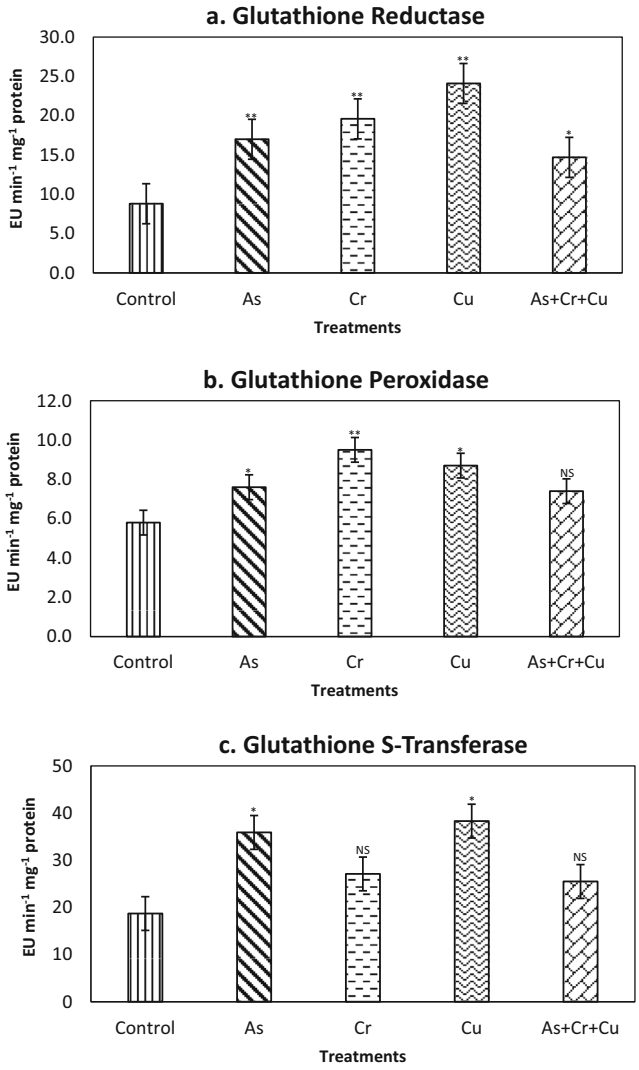

Fig. 6 Changes in the activity of **a** glutathione reductase (GR), **b** glutathione peroxidase (GPX), **c** glutathione S-transferase (GST) at 7 days after treatment (DAT) under different metal stresses. Values are mean of triplicates (± S.E), $*P \leq 0.05$, $**P \leq 0.01$; NS, non-significant

stress increased PC content from 313.5 (control) to 420 (+ 34%), 407 (+ 30%), 473 (+ 51%), and 407 (+ 30%) nmoles g^{-1} FW respectively (Fig. 7a). Similarly, NPT content also increased in each treatment. In the plants exposed to As, Cr, and Cu and their combined stress, the content of NPT increased from 358 (control) to 478 (+ 34%), 482 (+ 35%), 541 (+ 51%), and 457 (28%) nmoles g^{-1} FW, respectively (Fig. 7b).

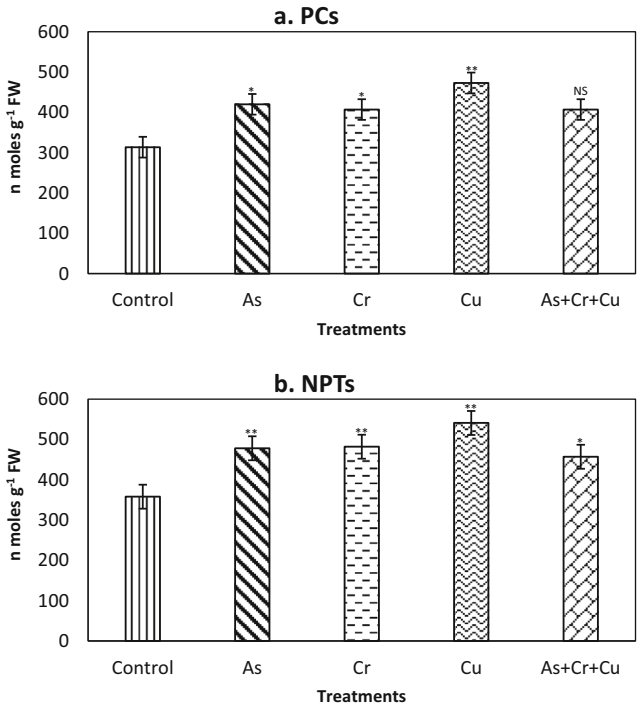

Fig. 7 Changes in the content of phytochelatins (**a**, PCs) and non-protein thiols (**b**, NPTs) at 7 days after treatment (DAT). Values are mean of triplicates (± S.E), $*P \leq 0.05$, $**P \leq 0.01$; NS, non-significant

Protein profiling through SDS-PAGE

An attempt was made to know the key proteins synthesized by the plants during stress; analyses was done by SDS-PAGE. The protein profiles of control and metal-treated leaves of *B. juncea* were compared at 7 DAT. The significant variations in the pattern of the protein profile were detected (Fig. 8a, b). Protein bands with a molecular weight extending from 14 to 97 kDa were observed in the present study. As a whole, about 29 bands of protein (1 to 29; Fig. 8b) were recognized and their intensities were further compared utilizing software Lab Image™ (Shown in the Supplementary Information (S2A–G). Under the given set of treatments, there was no total silencing or no new induction of proteins. In general, all stresses altered the protein profile of mustard leaf. Specifically, the abundance of eight protein bands (96.7 to16.6 kDa) was high in chromium and copper stress then in control. Band intensity of proteins was reduced in arsenic and combined stress except for the intensity of one protein band of 16.0 kDa (high then others) and 14.4 kDa (high then others) respectively. Six protein bands were selected on the basis of high induction in particular treatment then controls (Fig. 8a) for MALDI-TOF/TOF MS analysis. Protein band nos. 3, 9, and 22 (Fig. 8a; 64.4, 41.3, and 16.5 kDa) were overexpressed in both Cr- and Cu-treated plants than in control which are highly homologous to the mediator of RNA polymerase II transcription subunit 1 isoform X1 protein, chloroplastic ribulose-1, 5-bisphosphate carboxylase/oxygenase large subunit, and zinc finger A20/AN1 domain-containing stress-associated protein 5-like respectively, whereas protein band nos. 17 (Fig. 8a; 19.6 kDa) were overexpressed in only Cr-treated plants which are homologous to S3 ribosomal protein of chloroplast. Meanwhile, protein band nos. 23 and 29 (Fig. 8a; 16.0 and 14.4 kDa) were only upregulated under As and combined stress,

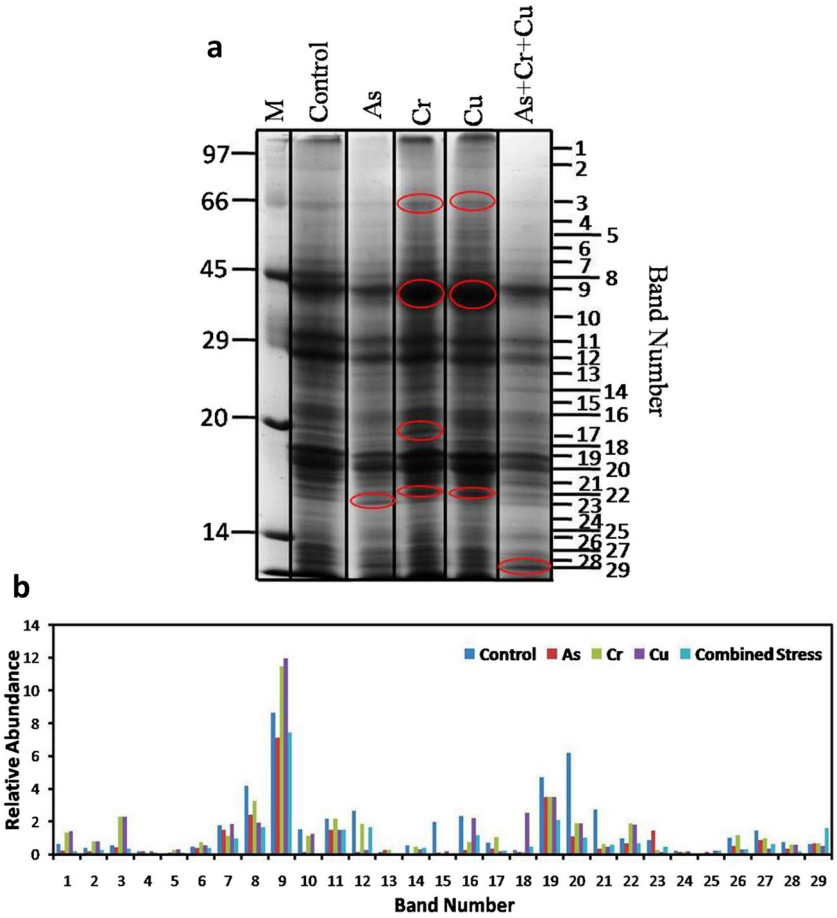

Fig. 8 **a** SDS-PAGE protein profile of *B. juncea* leaves after 7 days of As, Cr, and Cu and their combined stress. M (kDa) size marker. **b** Relative quantitative assessments of protein bands (1–29) of SDS-PAGE

respectively. Protein band nos. 23 and 29 were homologous to 15.7-kDa heat shock protein and autophagy protein 5–like respectively. Some important pieces of information of the identified proteins are shown in Table 2.

Multiple correlation analysis

Multiple correlation analysis was executed to analyze the interdependence of S-rich compounds, enzymatic antioxidants,

Table 2 List of different features of proteins excised from SDS-PAGE gel from band nos. 3, 9, 17, 22, and 23 and band no. 29 and identified by MALDI-TOF TOF/MS and MASCOT/UniProt

Band ID *	Homologous protein	Homologous organism	Location	MW (kDa): theoretical/ practical	Sequence length (AA)	No. of matched peptides	Mascot score
3	Mediator of RNA polymerase II transcription subunit 1 isoform X1	*Citrus clementina*	Nucleus	65.2 64.4	614	6	65
9	Ribulose-1,5-bisphosphate carboxylase/oxygenase large subunit	*Eclipta prostrata*	Chloroplast	45.8 40.4	411	8	96
17	Ribosomal protein S3	*Aphyllanthes monspeliensis*	Chloroplast	25.6 19.6	220	5	46
22	Zinc finger A20 and AN1 domain-containing stress-associated protein 5-like	*Elaeis guineensis*	Nucleus	16.5 16.5	145	4	54
23	15.7-kDa heat shock protein	*Solanum pennellii*	Peroxisome	16.1 16.0	145	5	64
29	Autophagy protein 5-like	*Dorcoceras hygrometricum*	Cytoplasm	13.9 14.4	122	6	49

*Band ID corresponding to the SDS-PAGE gel mentioned in Fig. 9a

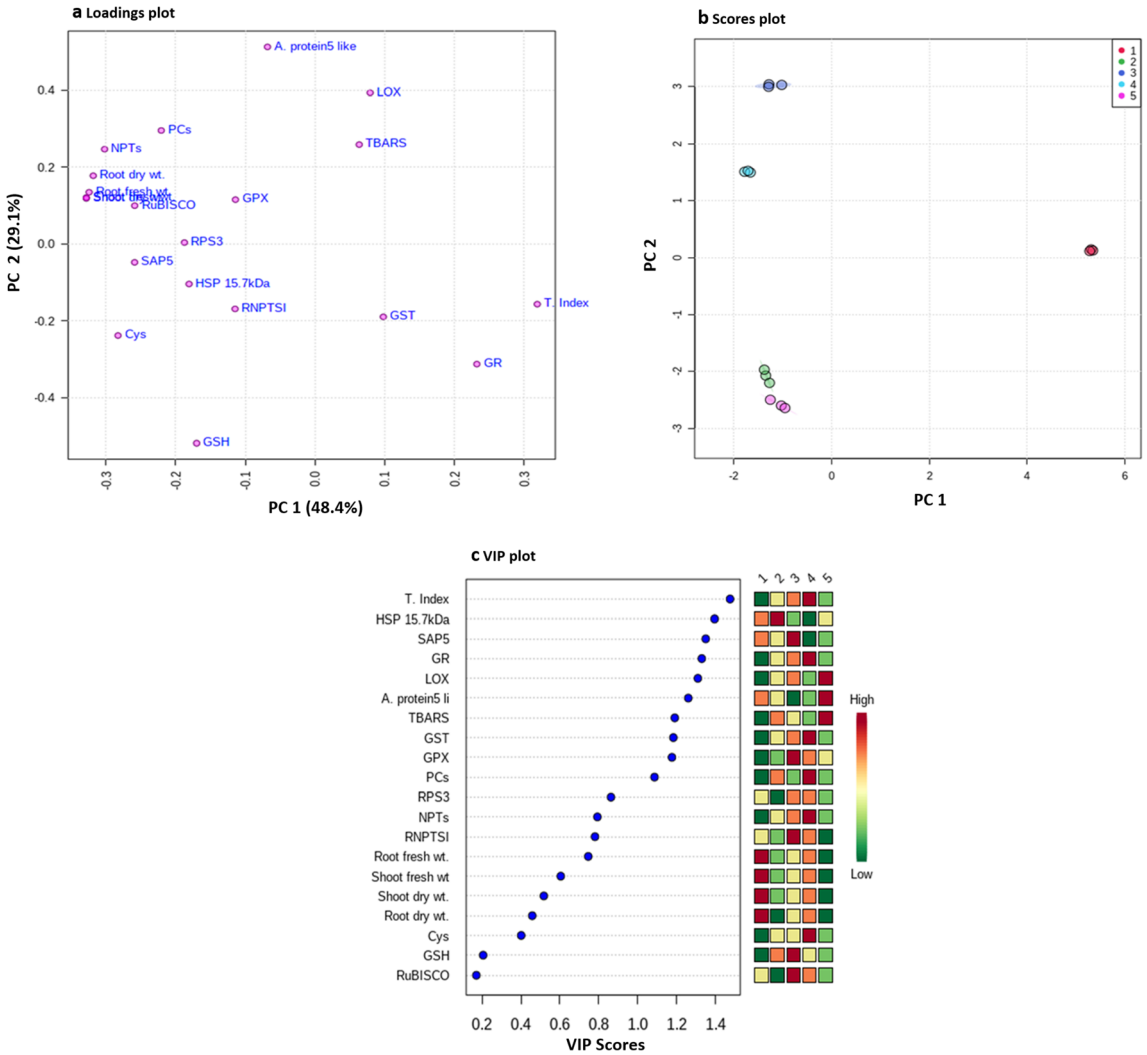

Fig. 9 Multiple correlation analyses of the information found in current study using MetaboAnalyst software. **a** Loading and **b** scatter plots of PCA study demonstrating a relationship among diverse metabolites, proteins, and antioxidants. Variable importance in projection (VIP) plot showing **c** metabolites, proteins, and antioxidants with the highest variation in *B. juncea*

proteins, tolerance index, and biomass under As, Cr, and Cu and their combined stress (Fig. 9a–c). Prior to the analyses of data utilizing the MetaboAnalyst software, the change in percentage for all constituent was log-transformed to base 2 for normalizing the scale of abundance. The unsupervised principal component analyses (PCA) and score plot permitted the data visualization and comparison of metabolites that are differentially modulated in *B. juncea* (Fig. 9a, b). The whole values of the physiological change 48.4% of variance were extracted from the first principal component axis (PC1) whereas 29.1% variance was extracted from the second PC axis (PC2) in leaf samples of *B. juncea* under metal(loid) stress. The score plot indicates clear separation by PC2 between the As and combined stress with Cr and Cu stress in plants. All the treated groups were well-segregated from the control by PC1. The TBARS and LOX, PCs and NPTs, and GST and GR activities in leaves were gathered close to each other. However, other metabolites of *B. juncea* appeared dispersed in loading plots presenting their altered performance under different treatments of metal(loid)s. Variable importance in the projection (VIP) plot was made based on the PLS-DA loading plots (Fig. 9c) to recognize the metabolites in *B. juncea* with a maximum abundance. A total of 20 constituents having VIP scores (0.10–1.5) were identified utilizing the VIP plots. Under metal stress in *B. juncea*, biomass was found to decrease (Fig. 10c, marked in green), whereas the antioxidant enzymes, proteins (such as RNPTS1, SAP5, RUBISCO, RPS3, HSP15.7 kDa, and ATG 5–like in particular stress), and S-rich compounds increased (Fig. 9c, marked in red and towards red) suggesting that the upregulation of these molecules plays an essential role in the defense system during stress.

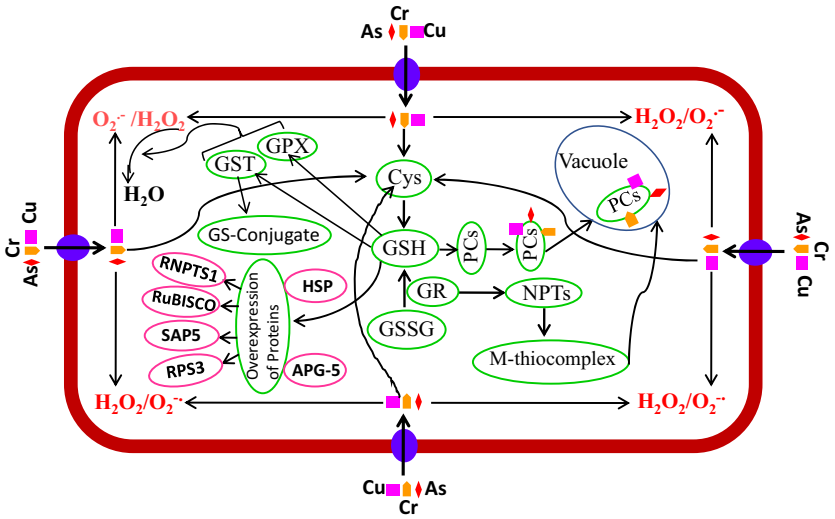

Fig. 10 Diagrammatic representation of a proposed biochemical processes underlying Indian mustard in response to As, Cr, and Cu and their combined stress. *Abbreviations*: RNPTS1, RNA polymerase II transcription subunit 1 isoform X1; RuBisCO, ribulose-1, 5-bisphosphate carboxylase/oxygenase large subunit; SAP5, stress-associated protein 5–like (zinc finger A20/AN1 domain-containing protein); RPS3, ribosomal protein S3; HSP, heat shock protein; APG-5, autophagy protein 5–like; GST, glutathione S-transferase; GSH, reduced glutathione; GSSG, oxidized glutathione; GR, glutathione reductase; Cys, cysteine; NPTs, non-protein thiols; PCs, phytochelatins

Discussion

As, Cr, and Cu accumulation in *B. juncea* cv. Pusa Jai Kisan

The concentration of As, Cr, and Cu in roots and shoots increased on the exposure of metals. However, the accumulation of such metals was very high in roots and shoots. The high accumulation of As, Cr, and Cu in the roots may be the result of efficient immobilization of these metals in the root cell vacuoles (do Nascimento et al. 2018). In addition, excessive metal ions found in the root cells might be due to its ability to bind strongly at the ion exchange sites of the cell wall and thus blocking its movement through the apoplastic pathway (Gautam and Dubey 2018). The movement of metals through endodermis is restricted by the Casparian strips also (Aleamotua et al. 2019). In our study, roots and shoots of *B. juncea* accumulated a larger amount of Cu then As followed by Cr. Such disparity reflects that plants have differential uptake mechanisms for different metals. These results suggest Cu uptake by the roots of Indian mustard, through COPT/Ctr protein transporters, is more efficient then phosphate transporter–mediated As uptake and carriers of essential anion–mediated Cr uptake (Franić and Galić 2019).

The solubility of metals in water also plays an important role in metal uptake (Ahmad et al. 2019a, b). Cu showed more uptake by the roots; perhaps this was due to good water solubility of Cu than As and Cr. However, in the presence of combined stress of As, Cr, and Cu, reduced accumulation of Cu in root as well as shoots demonstrated that As and Cr interfered with Cu uptake in *B. juncea*. On the other hand, co-existing As, Cr, and Cu stimulated the accumulation of As and Cr in both roots and shoots of *B. juncea*. Metal(loid) concentration in shoots of *B. juncea* was lower than in roots. Therefore, TF values were found to be < 1 (Table 1) suggesting that large amount of As, Cr, and Cu was restricted in roots and a smaller quantity is translocated to the aerial parts that are most remarkable for phytostabilization (Nouri et al. 2011). In this study, the accumulation of metals was also assessed through the bioconcentration factor (BCF). The values of BCF were found to be greater in root parts than in leaves with the exposure of As, Cr, and Cu and their combined stress. The BCF > 1 was observed for Cu and makes it clear that hydroponically *B. juncea* could accumulate Cu predominantly.

Oxidative stress and tolerance ability of *B. juncea*

As (non-redox active), Cr, and Cu (both are redox-active metals) and their combined stress to *B. juncea* resulted in oxidative stress via the excessive production of ROS, LOX activity, and lipid peroxidation. Lipid peroxidation is thought to be a marker of oxidative stress (Ahmad et al. 2017). In this study, the elevated levels of TBARS and LOX activity in leaf showed metal generated oxidative damage of the membrane lipids and other biomolecules (Hasanuzzaman et al. 2019). As and combined stress-induced lipid peroxidation was greater than the Cr and Cu stress. This could be due to the high production of ROS and LOX activity under these circumstances. It is evident that *B. juncea* can either neutralize the free radicals or employ various other scavenging processes to give better defense

against the oxidative stress induced by Cr and Cu stress. Indeed, the elevated level of the oxidative damage in *B. juncea* is additionally supported by histochemical staining of ROS. As described in various plant species, the whole fitness of plants is reflected by the accumulation of biomass (Li et al. 2018; Pan et al. 2019). Oxidative stress leads to the retardation of plant growth by disrupting the physiology as well as metabolism (Ahmad et al. 2018a, b). In *B. juncea*, the accumulation of fresh weight and dry weight was found to be reduced under As, Cr, and Cu and their combined stress. However, it was greatly declined in As and combined stress which was correlated with a high degree of oxidative stress of same plants. *B. juncea* behaved differently under Cr and Cu stress, showed better capability of plants to endure the oxidative damage (less reduction of biomass), and may be associated with higher production of sulfur-rich compounds, antioxidants, and some specific proteins (Ahmad et al. 2018a, b; Hasanuzzaman et al. 2018). Furthermore, based on root length under As, Cu, and Cr and their combined stress, the tolerance or growth index was calculated and compared with each other. Roots are the primary site of metal toxicity and thus might be a good indicator to assess the metal-generated oxidative damage. The present study demonstrates that As and combined stress of metals were more noxious to the root growth rather than the Cr and Cu stresses.

Shift of glutathione and its allied enzymes

In the current study, the level of endogenously present glutathione (GSH) was found to be increased in As, Cr, and Cu and their combined stressed plants than control plants. The elevated level of glutathione participating in the metal chelation acts as a powerful antioxidant and linked with the other important molecules under stress (Huang et al. 2019). For various vital enzymes of GSH metabolism such as GSTs and GPXs, glutathione acts as a substrate for them and itself serves as a reductant of disulfide to protect the enzyme thiol (-SH) groups (Ahmad et al. 2018a, b). In our study, increased glutathione content boosted GR, GST, and GPX activities under each stress condition except combined stress. GPX reduces H_2O_2 to H_2O and GST detoxifies organic hydroperoxides but both enzymes utilize GSH as the reducing agent. Furthermore, GSH is regenerated through the reduction of GSSG with the help of enzyme GR. Hence, our results are substantiated by Maresca et al. (2017).

Role of other S-rich compounds

S-containing compounds other than glutathione (GSH), phytochelatins (PCs), total non-protein thiols (NPTs), and cysteine (Cys) are also significant players in the defense of plants to toxic metal(loids) (Ahmad et al. 2019a, b). Cysteine availability in plants is mediated via GSH, GR, GPX, and GST in each metal stress condition jointly worked as ROS scavenger and reduced oxidative stress in *B. juncea*. Various pathways of sulfate assimilation operate as a source of reduced sulfur. This form of sulfur helps the synthesis of various S-rich compounds including MTs, PCs, and NPTs (Shen et al. 2019).

In our study, the level of cysteine was increased under As, Cr, and Cu and their combined stress. Moreover, the elevated level of cysteine was maximum under Cu stress. Cui et al. (2019) observed in their study that Cu existed as thiols (glutathione and cysteine) complex species in root tissues demonstrating the connection of Cu, glutathione, and cysteine. The thiol-rich peptides are known as phytochelatins; the concentration of phytochelatins was also increased in all sets of treatments, particularly in Cu stress. The increased level of PCs further activates the detoxification pathway in which these PCs attached to the heavy metals and form complexes which gets sequestered in the cell vacuoles (Ahmad et al. 2019a, b). In our study, under Cu stress, the amount of glutathione was found to be less in the leaf tissue than in Cr-treated plant's leaf which suggests that the greater fraction of this glutathione in root tissue is employed in the PCs' formation that leads to the greater Cu accumulation in the *B. juncea* roots. Similarly, NPTs are too important in plants under metal toxicity, the compounds which consist of various sulfhydryl acid-soluble components (Gratão et al. 2019). In the current investigation, the total content of NPTs increased by As, Cr, and Cu and their combined stress justifying their role in the detoxification of toxic metals. These observations indicate the role of PCs, NPTs, and Cys along with the glutathione which works synchronously in *B. juncea* to fight against the metal toxicity.

Modulation of protein pattern

To visualize the primary changes in the pattern of polypeptides under stress, SDS-PAGE is commonly used (Ahmad et al. 2019a, b). The protein cleanup process helps to remove high abundant proteins and enriching low abundant ones. Our results showed that proteins were differentially expressed (overexpressed/underexpressed) in Cr and Cu stress treatments than controls. However, As and combined stress caused more reduction in polypeptides' intensity compared with controls, possibly due to the degradation of several proteins. Proteins accumulated in higher amount might be the stress proteins playing crucial roles in the physiological adjustment under metal toxicity (Bagheri et al. 2017). Furthermore, some protein bands selected (nos. 3, 9, and 22 overexpressed in both Cr and Cu stress and nos. 17, 23, and 29 overexpressed in Cu, As, and combined stress, respectively) based on high induction for mass spectrometry analysis (Fig. 9a, b). The identified protein (band no. 3) was found to be the mediator of RNA polymerase II transcription subunit 1 isoform X1 which

functions as the co-regulator of the transcription of RNA polymerase II–dependent genes (Du et al. 2018).

Another identified protein was ribulose-1, 5-bisphosphate carboxylase/oxygenase large subunit (band no. 9) that is a key enzyme involved in the first step of carbon assimilation during the Calvin cycle (Gao et al. 2019). Band no. 22 was confirmed as zinc finger A20/AN1 domain-containing stress-associated protein 5–like usually activated in response to abiotic stresses (Baig et al. 2018). In addition, band no. 17 was revealed as S3 ribosomal protein of chloroplast. This protein is the constituent of ribosomal chloroplast, which is accountable for the chloroplast genome-encoded protein synthesis (Wang et al. 2016). On the other hand, band no. 23 was highly induced in As-stressed plants and identified as 15.7-kDa heat shock protein. A group of small proteins such as Hsp 15.7 kDa acts as a molecular chaperone and prevents protein aggregation as well as denaturation and therefore preserves the normal functions of proteins in cells under stress conditions (Ahmad et al. 2017). Interestingly, band no. 29 was well-expressed in combined stress only and identified as autophagy protein 5–like which is involved in the autophagy process. This was clearly indicating the activation of autophagy and suggesting the importance of this process to maintain the nutrient and energy resources during combined stress (Zhu et al. 2015). The up-regulation of proteins observed in this study comes through the proteome analyses during the toxic metal contamination probably in an effort by the plants to stimulate resistance strategies in response to metal stress. In summary, this study well demonstrates the relation of metal toxicity with the modulation of sulfur-rich compounds, changes in proteome and glutathione-related enzymes in Indian mustard under As, Cr, and Cu and their combined stress. A proposed biochemical mechanism was used by Indian mustard in response to metal(loid) stress (Fig. 10).

Conclusion

In this study, we investigated the As, Cr, and Cu and their combined effects on metal uptake and biochemistry of *B. juncea*. Our results suggest that metal absorption by *B. juncea* was affected in the presence of other metals. Co-existing As, Cr, and Cu stimulated the accumulation of As and Cr while discouraging the Cu in both roots and shoots of plants. *B. juncea* was effective in taking large amounts of Cu followed by As then Cr during individual exposure of metal(loid)s; however, it was not effectively transported to the shoots. Therefore, the roots of *B. juncea* execute a key function in metal retention to prevent toxic accumulation in the shoots. Exposure of As, Cr, and Cu and their combined toxicity induced oxidative stress, while it was more under combined stress. Metal toxicity, at certain levels, can promote the synthesis of glutathione and its related enzymes along with other S-rich compounds in *B. juncea* thus helping the survival of plants under toxicity of metal(loid)s. Among all the metal-treated plants, the concentration of such compounds was more pronounced in Cu-treated plants and resulted in higher resistance as evident from fresh and dry weight accumulation and less oxidative stress. Furthermore, identified proteins induced by Cr and Cu stress are associated with photosynthesis, transcription, and stress-related as they point to the function of such proteins in imparting stress tolerance against metal stress.

Acknowledgments Metal analysis in plant samples facilitated by Central Pollution Control Board, New Delhi, India, is appreciatively acknowledged.

Funding information This work is supported by King Saud University, Riyadh, Saudi Arabia through researchers supporting Project Number RSP-2020/186.

Compliance with ethical standards

Conflict of interest The authors declare that they have no conflict of interests

References

Ahmad J, Arif M, Bhajan R, Taj G (2009) Assessment of genetic diversity and genetic relationships among twenty varieties of *Brassica juncea* L. using RAPD markers. Int J Biotech Biochem 5(1):85–92

Ahmad J, Khan S, Khan GT (2012) Comparative assessment of genetic diversity among twenty varieties of *Brassica juncea* [L.] Czern & Coss using RAPD and ISSR markers. South Asian J Expt Bio 2(4): 166–176

Ahmad J, Bashir H, Bagheri R, Baig A, Al-Huqail A, Ibrahim MM, Qureshi MI (2017) Drought and salinity induced changes in eco-physiology and proteomic profile of *Parthenium hysterophorus*. PLoS One 12(9):e0185118

Ahmad J, Bagheri R, Bashir H, Baig M, Al-Huqail A, Ibrahim MM, Qureshi MI (2018a) Organ-specific phytochemical profiling and antioxidant analysis of *Parthenium hysterophorus* L. Biomed Res Int 2018:ID9535232

Ahmad J, Baig MA, Ali AA, Al-Huqail AA, Ibrahim MM, Qureshi MI (2018b) Differential antioxidative and biochemical responses to aluminium stress in *Brassica juncea* cultivars. Horticulture Env Biotech 59(5):615–627

Ahmad J, Ali AA, Baig MA, Iqbal M, Haq I, Qureshi MI (2019a) Role of phytochelatins in cadmium stress tolerance in plants. In: cadmium toxicity and tolerance in plants. Acad Press, pp 185–212

Ahmad J, Baig MA, Ali AA, Qureshi MI (2019b) Proteomics of cadmium tolerance in plants. In: Cadmium Tolerance in Plants. Acad Press, pp 143–175

Aleamotua M, McCurdy DW, Collings DA (2019) Phi thickenings in roots: novel secondary wall structures responsive to biotic and abiotic stresses. J Exp Bot 39:538–548

Ali H, Khan E, Ilahi I (2019) Environmental chemistry and ecotoxicology of hazardous heavy metals: environmental persistence, toxicity, and bioaccumulation. J Chemother 2019:ID 6730305

Anderson ME, Powrie F, Puri RN, Meister A (1985) Glutathione monoethyl ester: preparation, uptake by tissues, and conversion to glutathione. Arch Biochem Biophys 224

Bagheri R, Ahmad J, Bashir H, Iqbal M, Qureshi MI (2017) Changes in rubisco, cysteine-rich proteins and antioxidant system of spinach (*Spinacia oleracea* L.) due to sulphur deficiency, cadmium stress and their combination. Protoplasma 254(2):1031–1043

Baig MA, Ahmad J, Bagheri R, Ali AA, Al-Huqail A, Ibrahim MM, Qureshi MI (2018) Proteomic and ecophysiological responses of soybean (*Glycine max* L.) root nodules to Pb and Hg stress. BMC Plant Biol 18(1):283

Candiano G, Bruschi M, Musante L, Santucci L, Ghiggeri GM, Carnemolla B, Orecchia P, Zardi L, Righetti PG (2004) Blue silver: A very sensitive colloidal Coomassie G-250 staining for proteome analysis. Electrophoresis 25:1327–1333

Cui J-L, Zhao Y-P, Lu Y-J, Chan T-S, Zhang L-L, Tsang DCW, Li X-D (2019) Distribution and speciation of copper in rice (*Oryza sativa* L.) from mining-impacted paddy soil: Implications for copper uptake mechanisms. Environ Intl 126:717–726

do Nascimento JL, de Almeida AAF, Barroso J, Mangabeira PA, Ahnert D, Sousa AG, Baligar VC (2018) Physiological, ultrastructural, biochemical and molecular responses of young cocoa plants to the toxicity of Cr (III) in soil. Ecotoxicol Environ Saf 159:272–283

Doderer A, Kokkelink I, Van der Veen S, Valk BE, Schram AW, Douma AC (1992) Purification and characterization of two lipoxygenase isoenzymes from germinating barley. Biochim Biophys Acta 1120(1):97–104

Du J, Guo S, Sun J, Shu S (2018) Proteomic and physiological analyses reveal the role of exogenous spermidine on cucumber roots in response to $Ca(NO_3)_2$ stress. Plant Mol Biol 97(1–2):1–21

Elia AC, Galarini R, Taticchi MI, Dorr AJM, Mantilacci L (2003) Antioxidant responses and bioaccumulation in Ictalurusmelas under mercury exposure. Ecotoxicol Environ Saf 55:162–167

Foyer CH, Halliwell B (1976) The presence of glutathione and glutathione reductase in chloroplasts: a proposed role in ascorbic acid metabolism. Planta 133:21–25

Franić M, Galić V (2019) As, cd, Cr, Cu, Hg: Physiological implications and toxicity in plants. In: Plant Metallomics and Functional Omics, pp 209–251

Gaitonde MA (1967) Spectrophotometric method for the direct determination of cysteine in the presence of other naturally occurring amino acids. Biochem 104:627–633

Gao M, Yang Y, Song Z (2019) Effects of graphene oxide on cadmium uptake and photosynthesis performance in wheat seedlings. Ecotoxicol Environ Saf 173:165–173

Gautam A, Dubey RS (2018) Metal toxicity in plants: induction of oxidative stress, antioxidative defense system, metabolic alterations and phytoremediation. In: Hemantrajan (ed) Molecular physiology of abiotic stresses in plant productivity. Scientific Publishers, Jodhpur, pp 256–290

Gonzaga MIS, da Silva PSO, de Jesus Santos JC, de Oliveira Junior LFG (2019) Biochar increases plant water use efficiency and biomass production while reducing Cu concentration in *Brassica juncea* L. in a Cu-contaminated soil. Ecotoxicol Environ Saf 183:109557

Gratão PL, Alves LR, Lima LW (2019) Heavy metal toxicity and plant productivity: role of metal scavengers. In: Plant-Metal Interactions, pp 49–60

Habig WH, Pabst MJ, Jakoby WB (1974) Glutathione S-transferases. The first enzymatic step in mercapturic acid formation. J Biol Chem 249(22):7130–7139

Hasanuzzaman M, Hossain MS, Bhuyan MB, Al Mahmud J, Nahar K, Fujita M (2018) The role of sulfur in plant abiotic stress tolerance: molecular interactions and defense mechanisms. In: Plant Nutrients and Abiotic Stress Tolerance, pp 221–252

Hasanuzzaman M, Alam MM, Nahar K, Mohsin SM, Bhuyan MB, Parvin K, Fujita M (2019) Silicon-induced antioxidant defense and methylglyoxal detoxification works coordinately in alleviating nickel toxicity in *Oryza sativa* L. Ecotoxicology 28(3):261–276

Heath R, Packer L (1968) Photoperoxidation in isolated chloroplasts: I. Kinetics and stoichiometry of fatty acid peroxidation. Arch Biochem Biophys 125:189–198

Hoagland DR, Arnon DI (1950) The water-culture method for growing plants without soil. Circ Calif Agr Expt Sta 347

Howe G, Merchant S (1992) Heavy metal activated synthesis of peptides in *Chlymodomonas reinhartii*. Plant Physiol:127–136

Huang Y, Zhu Z, Wu X, Liu Z, Zou J, Chen Y, Cui J (2019) Lower cadmium accumulation and higher antioxidative capacity in edible parts of *Brassica campestris* L. seedlings applied with glutathione under cadmium toxicity. Environ Sci Pollut Res 26(13):13235–13245

Laemmli UK (1970) Cleavage of structural proteins during the assembly of the Head of Bacteriophage T4. Nature 227(5259):680–685

Javed MT, Tanwir K, Akram MS, Shahid M, Niazi NK, Lindberg S (2019) Phytoremediation of cadmium-polluted water/sediment by aquatic macrophytes: role of plant-induced pH changes. In: cadmium toxicity and tolerance in plants. Acad Press, pp 495–529

Li Z, Song Z, Yan Z, Hao Q, Song A, Liu L, Yang S, Xia S, Liang Y (2018) Silicon enhancement of estimated plant biomass carbon accumulation under abiotic and biotic stresses. A meta-analysis. Agron Sustain Dev 38(3):26

Lu Y, Wang QF, Li J, Xiong J, Zhou LN, He SL, Liu H (2019) Effects of exogenous sulfur on alleviating cadmium stress in tartary buckwheat. Sci Rep 9(1):7397

Marchiol L, Assolari S, Sacco P, Zerbi G (2004) Phytoextraction of heavy metals by canola (*Brassica napus*) and radish (*Raphanus sativus*) grown on multicontaminated soil. Environ Pollut 132(1):21–27

Maresca V, Sorbo S, Keramat B, Basile A (2017) Effects of triacontanol on ascorbate-glutathione cycle in *Brassica napus* L. exposed to cadmium-induced oxidative stress. Ecotoxicol Environ Saf 144: 268–274

Muszyńska E, Labudda M (2019) Dual role of metallic trace elements in stress biology-from negative to beneficial impact on plants. Int J Mol Sci 20(13):3117

Niazi NK, Bibi I, Fatimah A, Shahid M, Javed MT, Wang H, Ok YS, Bashir S, Murtaza B, Saqib ZA, Shakoor MB (2017) Phosphate-assisted phytoremediation of arsenic by *Brassica napus* and *Brassica juncea*: morphological and physiological response. Int J Phytoremediat 19(7):670–678

Nouri J, Lorestani B, Yousefi N, Khorasani N, Hasani AH, Seif F, Cheraghi M (2011) Phytoremediation potential of native plants grown in the vicinity of Ahangaran lead–zinc mine (Hamedan, Iran). Environ Earth Sci 62(3):639–644

Pan G, Zhang H, Liu P, Xiao Z, Li X, Liu W (2019) Effects of manganese stress on phenology and biomass allocation in *Xanthium strumarium* from metalliferous and non-metalliferous sites. Ecotoxicol Environ Saf 172:308–316

Paul M, Goswami C, Mukherjee M, Roychowdhury T (2019) Phytoremedial detoxification of arsenic by *Pistia stratiotes* and assessment of its anti-oxidative enzymatic changes. Bioremed J:1–10

Qadir S, Qureshi MI, Javed S, Abdin MZ (2004) Genotypic variation in phytoremediation potential of *Brassica juncea* cultivars exposed to Cd stress. Plant Sci 167:1171–1181

Qureshi MI, D'Amici GM, Fagioni M, Rinalducci S, Zolla L (2010) Iron stabilizes thylakoid protein–pigment complexes in Indian mustard during Cd-phytoremediation as revealed by BN-SDS-PAGE and ESI-MS/MS. J Plant Physiol 167(10):761–770

Rahman Z, Singh VP (2019) The relative impact of toxic heavy metals (THMs) (arsenic (As), cadmium (Cd), chromium (Cr)(VI), mercury (Hg), and lead (Pb)) on the total environment: an overview. Environ Monit Assess 191(7):419

Rizwan M, Ali S, ur Rehman MZ, Rinklebe J, Tsang DC, Bashir A, Maqbool A, Tack FMG, Ok YS (2018) Cadmium phytoremediation potential of Brassica crop species: a review. Sci Total Environ 631: 1175–1191

Safa M, O'Carroll D, Mansouri N, Robinson B, Curline G (2020) Investigating arsenic impact of ACC treated timbers in compost production (a case study in Christchurch, New Zealand). Environ Pollut 114218

Scarpeci TE, Zanor MI, Carrillo N, Mueller-Roeber B, Valle EM (2008) Generation of superoxide anion in chloroplasts of *Arabidopsis thaliana* during active photosynthesis: a focus on rapidly induced genes. Plant Mol Biol 66:361–378

Shen J, Su Y, Zhou C, Zhang F, Zhou H, Liu X, Yin X, Wu D, Yuan X (2019) A putative rice l-cysteine desulfhydrase encodes a true l-cysteine synthase that regulates plant cadmium tolerance. Plant Growth Regul:1–10

Šiukšta R, Bondzinskaitė S, Kleizaitė V, Žvingila D, Taraškevičius R, Mockeliūnas L, Čėsnienė T (2019) Response of *Tradescantia* plants to oxidative stress induced by heavy metal pollution of soils from industrial areas. Environ Sci Pollut Res 26(1):44–61

Su D, Jiang R, and Li H (2018). The potential of oilseed rape and *Thlaspi caerulescens* for phytoremediation of cadmium-contaminated soil. In twenty years of research and development on soil pollution and remediation in China 349-363

Thakur M, Udayashankar AC (2019) Lipoxygenases and their function in plant innate mechanism. In: Jogaiah S, Abdelrahman M (eds) Bioactive molecules in plant defense. Springer, Cham

Wang J, Yu Q, Xiong H, Wang J, Chen S, Yang Z, Dai S (2016) Proteomic insight into the response of *Arabidopsis* chloroplasts to darkness. PLoS One 11(5):e0154235

Watson BS, Asirvatham VS, Wang L, Sumner LW (2003) Mapping the proteome of barrel medic (Medicago truncatula). Plant Physiol 131(3):1104–1123

Xia J, Sinelnikov IV, Han B, Wishart DS (2015) MetaboAnalyst 3.0—making metabolomics more meaningful. Nucleic Acids Res 43: W251–W257

Zhu Y, Wang B, Phillips J, Zhang ZN, Du H, Xu T, Wang Z, Wang L, Deng X (2015) Global transcriptome analysis reveals acclimation-primed processes involved in the acquisition of desiccation tolerance in *Boea hygrometrica*. Plant Cell Physiol 56(7):1429–1441